Similar and Dissimilar Resistance Spot Welds of DP600 and X8Cr17 steels sheets: Welding Current and Fracture Toughness

Hassanen Jaber[1,2], Tünde Kovacs [3]

1-Doctoral School on Materials Sciences and Technologies, - Óbuda University, Hungary.

2- Engineering College, University of Thi-Qar, Nasiriyah, Iraq.

3-Donát Bánki Faculty of Mechanical and Safety Engineering- Óbuda University, Hungary.

hassen.jaber@bgk.uni-obuda.hu

Abstract — **This paper presents an experimental study on the fracture toughness in similar and dissimilar dual phase and ferritic stainless steel sheets. The sheet materials were joined by using resistance spot welding as a lap joint. Tensile-shear tests were applied to the welded specimens. The variation of the nugget diameter according to welding current was investigated. Also, the microhardness distribution was investigated. The results were discussed and plotted as graphs.**

Keywords: Fracture Toughness; Dual Phase Steel; Ferritic Stainless Steel; Resistance Spot Welding.

1 INTRODUCTION

Joints between dissimilar metals are particularly common in components used in the automotive industries, dissimilar welding represents a major scientific and technical challenge [1].

In 1994, an international consortium of sheet steel producers comprised of 35 companies from 18 countries started the Ultra Light Steel Auto Body project (ULSAB) to explore opportunities for weight saving in automotive components. The (ULSAB) project has shown that car body mass can be reduced by 25% and 14 % less cost using advanced high-strength steels (AHSS) and innovative processes [2,3]. It is anticipated that AHSS usage in automotive bodies will climb to 50% by 2015 [4].

Dual phase (DP) steels are one of the most common AHSS steels. DP steels, which consist primarily of a ductile ferrite phase and a strong martensite phase, provide excellent mechanical properties in commercial high-strength low-alloy steels. Compared with carbon steels, DP steels exhibit a number of unique mechanical properties such as slightly lower yield strength and more uniform and higher total elongation, which is responsible for their relatively good formability. These properties, combined with high strengths, have made DP steels attractive for automotive applications [5,6]. In recent years, DP600 applications are widely used in different automobile models such as Porsche Cayenne and VW Touareg [7]. Fig. 1 illustrates The automobile parts in which DP 600 steel is used [8].
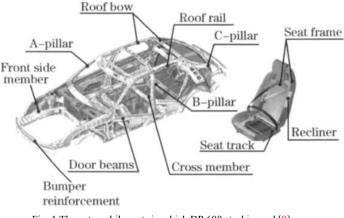

Fig. 1 The automobile parts in which DP 600 steel is used [8].

Although austenitic stainless steel has common use, ferritic stainless steel (X8Cr17) has many advantages. Firstly, ferritic stainless steels are more economic because they do not contain nickel which is an expensive alloy. Ferritic stainless steels have good corrosion resistance with good formability and ductility. They are magnetic and have low thermal expansion. Due to these advantages, X8Cr17 have been widely used in automotive components [9,10]. It is interesting to note that AISI 430 X8Cr17 is widely accepted for use in structural frameworks and body panelling of buses and coaches [11].

Resistance spot welding is a widely used and important welding process in automotive body construction because of its low cost, easy automation, minimum skill

requirements, and robustness to part tolerance variations. Typically, there are about 2000-5000 spot welds in a modern vehicle [12]. Mechanical properties and performance of resistance spot welded joints are generally considered under static or quasistatic loading condition. The tensile-shear is the most widely used tests for evaluating the spot weld mechanical performance in static conditions. More cracks and failures tend to occur around these welds, in the heat-affected zone (HAZ), because those joints are exposed to dynamic and static loads in the automobile structures [13].

Fatigue life for a spot weld is often expressed in terms of stress density, or stress intensity factor. These quantities are used to predict fatigue life of resistance spot welding. The factors such as shear stress acting in RSW zone, sheet thickness, multi pass welding, and the width of the welding zone are the important parameters that affect the performance of the joint[14]. The fracture of a material is studied in three different modes [15]. These are opening mode, sliding mode, and tearing mode, (Fig. 2) with associated intensity factors, where K_I, K_{II}, K_{III}, respectively. Pook [16] investigated the fracture behaviour of spot welds using the expressions developed by Paris, Sih, and Kassir [17, 18] based on elliptical connections, in spot-welded joints. Pook developed the stress intensity factor equation for spot weld.
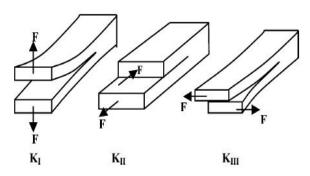

Fig. 2 Basic fracture modes: K_I opening mode; K_{II} shearing mode; K_{III} tearing mode [15]

$$K_{11} = \frac{F}{(D/2)^{3/2}} \left\{ 0.282 + 0.162 \left(\frac{D}{t}\right)^{0.710} \right\} (MPa.m^{0.5}) \qquad (1)$$
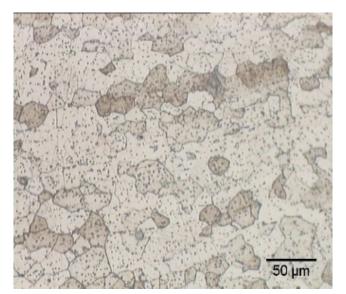
Where F is the tensile-shear force, D is the weld diameter, t is the sheet thickness. Zhang [19,20] studied the spot weld joints between sheets of dissimilar materials and different thickness. He found the relations between the J integrals and stress intensity factors for sheets of either the same thickness or different thickness. He offers equations to compute the stress intensity factors for spot welds of dissimilar materials.

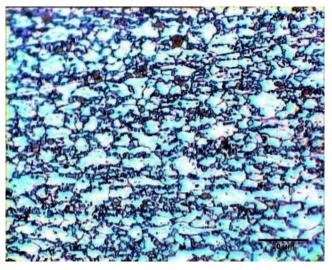$$K_{11} = \frac{2F}{\pi D \sqrt{t}} (MPa.m^{0.5}) \qquad (2)$$

Bae et al [21]. proposed a model for predicting fatigue life of the spot welds by considering the welding residual stresses. Their results showed that the fatigue limit calculated here is 25% less than the fatigue limit calculated without considering the residual stresses. Khan et al. [22] reported that the RSW fatigue performance of the dissimilar materials HSLA350/DP600 was similar to the fatigue performance of HSLA350/HSLA350.

2 EXPERIMENTAL PROCEDURE

A 1.5 mm thick DP600 dual phase steel and a 1.5 mm AISI 430 ferritic stainless steels sheets were used as the base metals. The initial microstructures of base metals are given in Fig. 3. The chemical composition of the base metals which was determined using a standard quantumeter were (0.07C, 1.52Mn, 0.008P, 0.011S, 0.048Si, 0.1Cr, 0.02 Mo, 0.02Mo, 0.01V, 0.005Nb, 0.05Cu) for DP600 and (0.05C, 0.48Mn, 0.028P, 0.005S, 0.28Si, 16.9Cr, 0.2Mo, 0.006V, 0.003Nb, 0.16Cu, 0.16Ni) for X8Cr17. The mechanical properties of the base metals were determined using a standard tensile test in accordance to ASTM E8M [23]. Table 2 shows the mechanical properties of the investigated steels. Resistance spot welding was performed using a PLC controlled, 120 kVA AC pedestal type resistance spot welding machine. Welding was conducted using a 45° truncated cone RWMA Class 2 electrode with 8 mm face diameter.

a: X8Cr17

b:DP600

Fig. 3. The initial microstructures of base metals.

Table (2) Mechanical properties of (DP600) and (X8Cr17).

	YS, MPa	UTS, MPa	EL, %
DP600	400	670	24
X8Cr17	330	490	33

*YS is yield strength; UTS is ultimate tensile strength; EL is elongation.

Welding process was carried out with a constant electrode pressure of 4 bar depending on specimen thickness. Squeeze, welding and holding time were kept constant at 45, 15 and 10 cycles, respectively. Welding current changed step by step from 6 to 13 kA. Three samples were spot welded for each current used for the tensile–shear tests.

In order to evaluate the fracture toughness of the spot welds, the tensile-shear test was performed. The tensile-shear test samples were prepared according to ANSI/ AWS/SAE/D8.9-2012 standard [24]. Fig. 4 shows the tensile-shear sample dimensions. The tensile-shear tests were performed at a cross head of 2 mm/min with a 20 ton Instron universal testing machine.
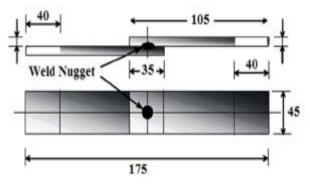

Fig. 4. Tensile-shear test sample dimensions (mm) [24]

The fracture force of the welded parts was determined from the data obtained in the tensile-shear tests. The nugget diameters were measured, where a minimum and maximum axes across these zones were measured using a digital calipers (Fig. 5). Three measurements were performed for each of the sample. Mean values of the measurements were taken as nugget diameter. Equation 1 and 2 were used to calculate the fracture toughness values (K_{IIC}) for similar and dissimilar resistance spot welds, respectively.
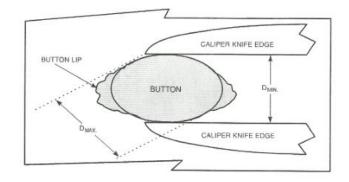

Fig (5): Technique for measuring fusion zone size [24].

3 RESULT AND DISCUSSION

As shown in Fig. 6, when the weld current is increased, the fracture toughness increases due to the increasing of fusion zone size and fusion penetration depth until a critical weld current. After that value, fracture toughness decreases

because of the expulsion at the faying interface shown in Fig. 7. Spot welds with expulsion exhibit severe decreasing of fusion zone size and fusion penetration depth.
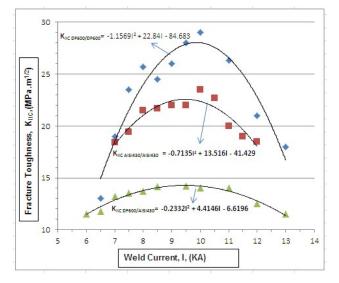

Fig. 6. Fracture toughness (K_{IIC}), versus weld current(I) for DP600/ DP600, X8Cr17/ X8Cr17 and DP600/ X8Cr17 RSW.

Fig. 7: Expulsion trace in the DP00/ X8Cr17 RSW.

The difference of fracture toughness of similar combinations (DP600/DP600 and X8Cr17/X8Cr17) comes from difference of base metal strength, microstructure of fusion zone (FZ), and hardness profiles of RSW zones.

Fig. 6 showed that the fracture toughness of the DP600/DP600 joint is (27 MPa.m$^{0.5}$) which is higher than that of the X8Cr17/X8Cr17 (23 MPa.m$^{0.5}$), due to the former's higher base metal strength (UTSDP= 670 MPa, UTSX8Cr17 = 490 MPa). On the other hand, fracture

toughness of dissimilar combinations DP600/ X8Cr17 is (18 MPa.m$^{0.5}$) which is lower than that of the similar combinations (DP600/DP600 and X8Cr17/ X8Cr17). The one reason for this result is heat unbalance between the steel sheets which occurs during spot welding operations of steel sheets having different material properties, especially electrical resistance. Due to the heat unbalance, the nugget between the sheets cannot occur symmetrically. Antisymmetric nugget formation decreases fracture toughness of the welded sheet combination as shown in Fig 8. The second reason is due to the fact that the equations using to compute the fracture toughness for spot welds of dissimilar materials difference form the equations using to compute the fracture toughness for spot welds of similar materials.

Fig. 9 shows the hardness profile of DP600/DP600, X8Cr17/X8Cr17 and dissimilar combination of DP600/X8Cr17. As can be seen in Fig. 8, the FZ hardness increases in order of X8Cr17/X8Cr17, DP600/ X8Cr17 and DP600/DP600. The difference in the FZ hardness of the similar and dissimilar combinations is influenced by the chemical composition and the microstructure of the FZ. Fig. 10 shows typical FZ microstructures of similar and dissimilar combinations. The chemical composition of the FZ is a mixture of the composition of each of the base metals. Hence, the FZ hardness is affected by the mixing/dilution degree of the base metals.
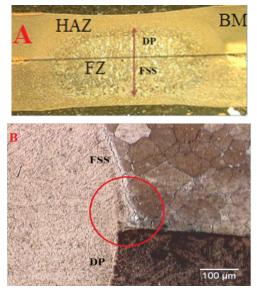

Fig. 8: **(a)** Typical macrostructure of DP/X8Cr17 resistance spot welds, **(b)** the joint region between DP and X8Cr17.
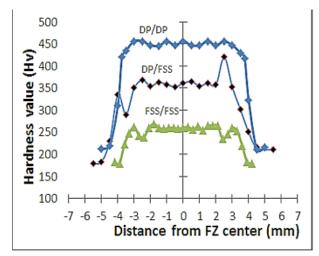
Fig (9): Typical hardness profiles of DP600/DP600, DP600/ X8Cr17 and X8Cr17/ X8Cr17 combinations.
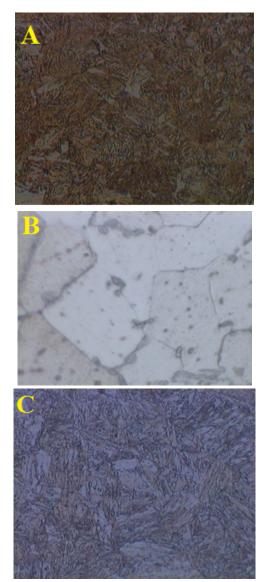

Fig. 10. Typical FZ microstructure of (a) DP600/DP600, (b) DP600/ X8Cr17 and (c) X8Cr17/ X8Cr17 RSWs.

CONCLUSIONS

1- Fusion zone size was proved to be key factor controlling mechanical properties of DP600/DP600, DP600/ X8Cr17 and X8Cr17/X8Cr17 welds in terms of fracture toughness and peak load.

2- Due to excessive welding heat input, where expulsion occurs, the peak load is significantly reduced. Significant reduction of failure energy can be attributed to the reduction of weld fusion zone at high welding current.

3- The fracture toughness of spot weld is not only dependent on the nugget diameter but also depends on sheet thickness, tensile rupture force, and welding current.

REFRENACE

[1] 1- M.M.A. Khan and L. Romoli, G. Dini, (2013). Laser beam welding of dissimilar ferritic/martensitic stainless steels in a butt joint configuration: *Optics & Laser Technology*, Vol 49, pp.125–136.

[2] American Iron and Steel Institute(AISI), (2006). *UltraLight Steel Auto Body*. ULSAB Final Report, Washington, DC.

[3] M. Marya and X. Q. Gayden. (2005). Development of Requirements for Resistance Spot Welding Dual-Phase (DP600) Steels Part 1 — The Causes of Interfacial Fracture: *Welding Journal*, Vol 84, pp. 173s-182s, November.

[4] M. Tumuluru, (2006). Resistance Spot Welding of Coated High-Strength Dual-Phase Steels: *Welding Journal*, (Miami, Fla), Vol 85, PP. 31-37, August.

[5] C. Ma, D.L. Chen, S.D. Bhole, G. Boudreau , A. Lee , E. Biro. (2008). Microstructure and fracture characteristics of spot-welded DP600 steel: *Materials Science and Engineering A* Vol 485, PP. 334–346.

[6] X. Sun, E. Stephens and M. Khaleel (2008). Effects of fusion zone size and failure mode on peak load and energy absorption of advanced high strength steel spot welds under lap shear loading conditions: *Engineering Failure Analysis*, Vol 15, pp. 356–367.

[7] H. Hofmann, D. Mattissen, T. W. Schaumann (2006). Advanced cold rolled steels for automotive applications: *Mat.-wiss. u. Werkstofftech*, Vol 37, No. 9, PP. 716-723.

[8] F. Hayat (2011). Comparing Properties of Adhesive Bonding Resistance Spot Welding and Adhesive Weld Bonding of Coated and Uncoated DP 600 Steel: *Journal Of Iron And Steel. Research, International.* Vol 18, No 9: PP. 70-78.

[9] Hoon-Hwe Cho, Heung Nam Han, Sung-Tae Hongb, Jong-Hwan Park, Yong-Jai Kwon, Seok-Hyun Kim, Russell J. Steel (2011). Microstructural analysis of friction stir welded ferritic stainless steel: *Materials Science and Engineering A* Vol 528, PP. 2889–2894.

[10] M. Bilgin , C. Meran (2012). The effect of tool rotational and traverse speed on friction stir weldability of AISI 430 ferritic stainless steels: *Materials and Design*, Vol 33, pp. 376–383.

[11] P. Snelgrove (2012). *Stainless steel automotive and transport developments.* International Stainless Steel Forum, www.worldstainless.org

[12] Ugur Ozsarac (2012). Investigation of Mechanical Properties of Galvanized Automotive Sheets Joined by Resistance Spot Welding: *Journal of Materials Engineering and Performance*, ASM International, Vol 21, PP. 748–755.

[13] M. Pouranvari, S.P.H. Marashi, D.S. Safanama (2012). Susceptibility to interfacial failure mode in similar and dissimilar resistance spot welds of DP600 dual phase steel and low carbon steel during cross-tension and tensile-shear loading conditions: *Materials Science and Engineering A* Vol 546, PP. 129– 138.

[14] I. Sevim (2006) Effect of hardness to fracture toughness for spot welded steel sheets: *Materials and Design*, Vol 27, pp.21–30.

[15] Lawn B (1993). *Fracture of brittle solids printed in Great Britain*, 2nd ed. Cambridge: University Press.

[16] Pook LP (1975) Fracture mechanics analysis of the fatigue behavior of spot welds. *Int J Fract* 11:173–176.

[17] Paris PC, Sih GC (1965) *On fracture toughness testing and its application*, ASTM STP381. ASTM, Philadelpia, p30.

[18] Kassir MK, Sih GC (1968) *Int J Fract Mech* 41:347–353.

[19] Zhang D. (1997). Stress intensities at spot welds. *Int J Fract* ;88:167–85.

[20] Zhang D. (1999). Stress intensities derived from stresses around a spot weld. *Int J Fract* ;99:239–57.

[21] D. H. Bae, I. S. Sohn and J. K. Hong (2003). Assessing the effects of residual stresses on the fatigue strength of spot welds:, *Weld J*, 82, 18s–23s.

[22] Khan MS, Bhole SD, Chen DL, Biro E, Boudreau G, Deventer J (2009). Welding behaviour, microstructure and mechanical properties of dissimilar resistance spot welds between galvannealed HSLA350 and DP600 steels: *Sci Technol Weld Join* 14:616–25.

[23] Standard Methods of Tension Testing of Metallic Materials, E 8. Annual book of ASTM standards, vol. 03.01. ASTM, Philadelphia; 2004.

[24] ANSI/AWS/SAE/D8.9-2012 " Test Method For Evaluating The Resistance Spot Welding Behavior of Automotive Sheet Steel Materials", American Welding Society, 2012.